DOI: 10.1002/ejic.200900417

Structural and Magnetic Study of a Trinuclear Mn^{II}–Gd^{III}–Mn^{II} Complex

Jean-Pierre Costes,*[a,b] Javier Garcia-Tojal,[c] Jean-Pierre Tuchagues,[a,b] and Laure Vendier[a,b]

Keywords: Manganese / Gadolinium / Structure elucidation / Magnetic properties

The synthesis, structural determination and magnetic study of a trinuclear Mn^{II}–Gd^{III}–Mn^{II} complex involving a Schiff base ligand are described. The structural study demonstrates that the complex presents a linear arrangement of the Mn and Gd ions, with hexacoordinate Mn ions in slightly distorted or distorted trigonal prism environments and nine-coordinate gadolinium ions. The Mn and Gd ions are linked by two phenoxido bridges for one Mn–Gd subunit and two phenoxido plus one nitrato bridges for the other Mn–Gd subunit. Ferromagnetic interactions operate in the complex. The best fit takes into account two different J constants and D and E zero-field splitting terms. A strict 3d-5d(Gd) orthogonality is not possible in the present complex because all 3d orbitals of the Mn ions are occupied, which does agree with the weak value of the $J_{Mn,Gd}$ parameter. Oxidation of this complex does not yield the corresponding Mn^{III}–Gd^{III}–Mn^{III} entity.

Introduction

Schiff base ligands have been largely used to assemble 3d and 4f ions and to yield di- or triheteronuclear 3d-4f complexes.[1–3] These low nuclearity complexes help to understand the magnetic behaviour of the 3d-4f complexes, and interpretation of their magnetism involves a unique J parameter. Moreover, an isotropic Hamiltonian may be used when gadolinium, with its half-filled 4f orbitals and its $^8S_{7/2}$ ground state, is associated to copper[1–3] or vanadyl ions.[4] Although analysis of the Ni–Gd,[5] Co–Gd[6] and Fe–Gd[7] complexes is complicated by the orbital contribution of the 3d ions, these heterodinuclear complexes do exist and also allow such studies. However, an equivalent Mn^{II}–Gd-Schiff base complex has never been synthesized. Our first attempt in this direction yielded an ionic species with two [Mn^{III}–Schiff base] complex cations surrounding a dianionic [$Gd(NO_3)_5(MeOH)$] entity without any direct bonding interaction between the Mn and Gd centres.[8] Since then, other ligands have been used to fill this gap. Ligands possessing carboxylate functions, such as EDTA,[9] glutaric[10] or chelidamic[11] acid have yielded 2D Ln_2Mn_3 or Ln_2Mn polymers, whereas pyridine-2,6-dicarboxylic acid[12] and oxodiacetic acid[13] have yielded 3D Ln_2Mn_3 structures. Clusters of variable nuclearities, Mn_6Ln_6, $Mn_{11}Ln_4$, Mn_3Ln_2, were isolated with salicylhydroxamic acid[14] or simple organic acids.[15,16] Except for the Mn_3Ln_2 cluster, the Mn ions are at different oxidation states, +3 and +4 for Mn_6Ln_6 and +2 and +3 for $Mn_{11}Ln_4$. More recently, complexes of lower nuclearities, Mn_2Ln_2 and Mn–Ln–Mn, were prepared with a thiacalix[4]arene[17] and a phosphorus-supported trishydrazone ligand.[18] In these later two examples the Mn^{II}–Gd^{III} entities were characterized. In the present study, we introduce the synthesis of the first trinuclear Mn^{II}–Gd–Mn^{II} complex prepared from a tetradentate Schiff base ligand, its structural determination and an interpretation of its magnetic properties.

Results

Manganese–gadolinium complex **1** crystallizes in the monoclinic space group $P2_1/n$ with $Z = 4$. The crystallographic data of complex **1** are collated in Table 1, whereas selected bond lengths and angles are mentioned in the figure caption. The structural determination of complex **1** evidences the existence of a trinuclear Mn–Gd–Mn complex molecule, as shown in Figure 1. This molecule may be formulated as [$(NO_3)Mn(L)(\mu\text{-}NO_3)Gd(L)Mn(NO_3)$]. Surprisingly, the nitrato anions are coordinated to the metal centres through three different coordination modes. One nitrato bridges gadolinium to Mn1 in a classical $\mu\text{-}\eta_1\text{-}\eta_1$ mode, a second one chelates Mn2, whereas the third one is coordinated to Mn1 in a monodentate η_1 fashion. The gadolinium centre is nine-coordinate to the four phenoxido and the four methoxy oxygen atoms of the two L ligands and to an oxygen atom of the bridging nitrato. The manganese ions are six-coordinate, both to the N_2O_2 coordination site of one L

[a] CNRS, LCC, Laboratoire de Chimie de Coordination, 205, route de Narbonne, 31077 Toulouse, France
E-mail: costes@lcc-toulouse.fr
[b] Université de Toulouse, UPS, INPT, LCC, 31077 Toulouse, France
[c] Departamento de Quimica, Universidad de Burgos, Misael Banuelos, s/n, 09001 Burgos, Spain
Supporting information for this article is available on the WWW under http://dx.doi.org/10.1002/ejic.200900417.

ligand and two oxygen atoms from NO_3 anions: one O from both the monodentate and the bridging NO_3 for Mn1, and two O from the chelating NO_3 for Mn2. The LMn1 moiety is not planar, but has an umbrella shape with both NO_3 pointing above; in contrast, the ligand around Mn2 is much less distorted. Mn1 and Mn2 are located 0.923(1) and 0.688(1) Å out of their mean N_2O_2 plane toward their coordinated nitrato anion, respectively. The corresponding Mn···Gd separations are equal to 3.516(1) and 3.709(1) Å, respectively. The angle between the two OGdO planes containing the bridging phenoxido oxygen atoms is equal to 73.7(1)° and the dihedral angles between the Mn1O1O2, GdO1O2 and Mn2O3O4, GdO3O4 planes are equal to 49.8(1) and 3.3(1)°, respectively. Nevertheless, the Mn1, Gd and Mn2 centres are practically aligned, with a Mn···Gd···Mn angle of 176.6(1)° and a Mn···Mn distance of 7.221(1) Å. Adjacent trinuclear units are well isolated from each other, with intermolecular Mn···Mn and Mn···Gd distances larger than 7.2 Å, and without any hydrogen-bonding interactions.

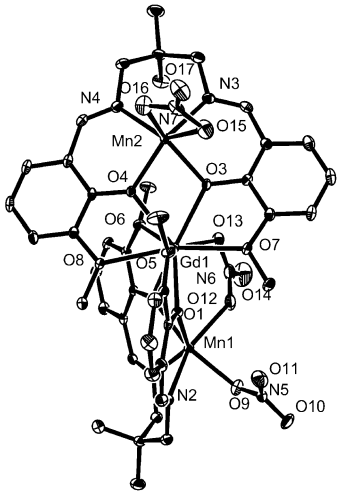

Figure 1. Molecular structure of the trinuclear complex $[(NO_3)Mn(L)(\mu\text{-}NO_3)Gd(L)Mn(NO_3)]$ (**1**) with thermal ellipsoids drawn at the 30% probability level. Hydrogen atoms are omitted for clarity. Selected bond lengths [Å] and angles [°] for **1**: N1–Mn1 2.232(5), N2–Mn1 2.256(5), N3–Mn2 2.178(5), N4–Mn2 2.168(5), O1–Mn1 2.187(4), O1–Gd1 2.330(4), O2–Mn1 2.210(4), O2–Gd1 2.373(4), O3–Mn2 2.092(4), O3–Gd1 2.376(4), O4–Mn2 2.116(4), O4–Gd1 2.398(4), O5–Gd1 2.574(4), O6–Gd1 2.535(4), O7–Gd1 2.593(4), O8–Gd1 2.590(4), O9–Mn1 2.206(5), O12–Mn1 2.175(5), O13–Gd1 2.357(5), O15–Mn2 2.409(6), O16–Mn2 2.241(6), Mn1–Gd1 3.5158(11); Mn1–O1–Gd1 102.17(15), Mn1–O2–Gd1 100.11(14), Mn2–O3–Gd1 112.07(17), Mn2–O4–Gd1 110.16(16), O1–Mn1–O2 72.21(14), O3–Mn2–O4 73.78(15), O1–Gd1–O2 66.85(13), O3–Gd1–O4 63.84(13).

The larger deformation of the Mn1 coordination sphere in comparison to that of Mn2 is corroborated by the Mn–N and Mn–O bond lengths, which are larger for Mn1 than for Mn2, 2.244 against 2.173 Å in average for Mn–N bonds and 2.198 against 2.104 Å in average for Mn–O bonds. Whereas the Gd–O bonds involving deprotonated phenoxido oxygen atoms [2.330(4) to 2.398(4) Å] are quite similar to those in other 3d-Gd complexes, the Gd–O bonds involving neutral methoxy oxygen atoms [2.535(4) to 2.590(4) Å] are shorter than usual. The shorter Mn–O bond [2.175(5) Å] involves the bridging nitrato, as compared to the monodentate [2.206(5) Å] and the chelating [2.241(6) and 2.409(6) Å] NO_3 anions. The coordination geometry around each Mn centre was analyzed with a continuous shape measure carried out with the SHAPE program,[19] confirming that Mn1 is closer to a regular trigonal prism [$S(D_{3h})$ = 1.4, $S(O_h)$ = 10.7], whereas Mn2 presents a larger deformation from a trigonal prism [$S(D_{3h})$ = 4.1, $S(O_h)$ = 13.1]. The S coefficient is the shape measure of the investigated Mn structure relative to an ideal shape, here trigonal prism or octahedron. It can vary from zero (ideal shape) to 100.

When a solution containing crystals **1** is taken out of the glove box, we observe a darkening of the solution and disappearance of the yellow crystals (Experimental Section). Three days later new (dark) crystals of complex **2** have formed. Although their structural determination is of low quality, it is sufficient to show that complex **2** is a mononuclear complex in which the Mn ion is equatorially chelated to the N_2O_2 coordination site of the ligand and axially coordinated to two water molecules (Figure 2). Although several Mn^{III} complexes made with very similar Schiff bases are known,[20,21] the present one has not been reported in the literature. Oxidation of the manganese ion, confirmed by the presence of a nitrate counteranion, is accompanied by loss of the Gd ion, thus showing that Mn^{III}–Ln^{III} complexes involving this tetradentate Schiff base cannot be prepared through the reported synthetic pathway.

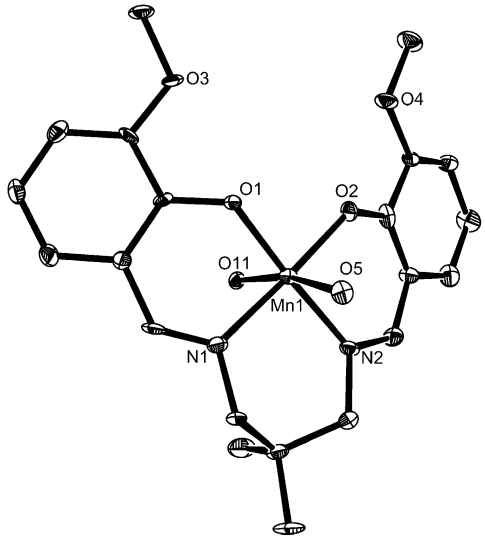

Figure 2. Molecular structure of the mononuclear cation $[(LMn(H_2O)_2]^+$ of **2**, with thermal ellipsoids drawn at the 30% probability level. Hydrogen atoms are omitted for clarity.

Magnetic Properties

The thermal variation of the $\chi_M T$ product for complex **1** is displayed in Figure 3; χ_M is the molar magnetic susceptibility of the trinuclear species corrected for the diamagne-

tism of the ligands. At 300 K, $\chi_M T$ is equal to 16.98 $cm^3 mol^{-1} K$, which corresponds to the value expected for uncoupled manganese (two) and gadolinium (one) ions (16.62 $cm^3 mol^{-1} K$ for $g = 2$). Lowering the temperature results in a slow increase in $\chi_M T$ down to 50 K (17.9 $cm^3 mol^{-1} K$) and then in a more abrupt one, up to 23.0 $cm^3 mol^{-1} K$ at 2 K. This behaviour indicates that a ferromagnetic interaction between the Mn^{II} ($S = 5/2$) and Gd^{III} ($S = 7/2$) ions operates at low temperature. A quantitative analysis has been performed on the basis of an expression derived from the effective spin Hamiltonian:[22]

$$\underset{i<j}{H} = -2\sum_{i,j} J_{ij} S_i S_j + \sum_i D_i S_{zi}^{\,2} + \sum_i E_i (S_{xi}^{\,2} - S_{yi}^{\,2}) + \beta H_z \sum_i g_{zi} S_{zi} + \beta H_x \sum_i g_{xi} S_{xi} + \beta H_y \sum_i g_{yi} S_{yi}$$

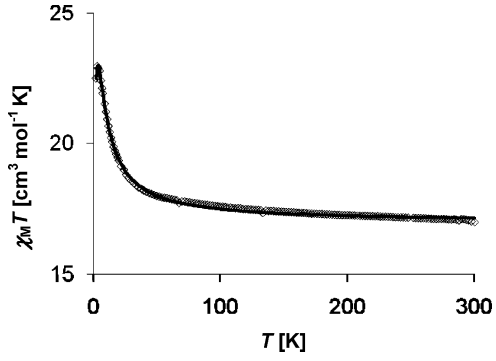

Figure 3. Temperature dependence of the $\chi_M T$ product for **1**. The line corresponds to the final fit 8 (see text) including zfs terms.

The magnetic susceptibility was computed by exact calculation of the energy levels associated with the spin Hamiltonian through diagonalization of the full energy-matrix. In order to take into account the large difference between the dihedral angles of the two MnOOGd cores, the possibility of two different interaction parameters J_1 and J_2 was considered. From the SHAPE analysis reported above, the Mn2 centre is essentially rhombically distorted, whereas Mn1 is essentially axially distorted. Consequently, the possibility of different axial zfs terms for Mn1 and Mn2 and also of a rhombic zfs contribution for Mn2 was also considered. According to literature data,[23–26] the possibility of zfs contribution for Gd was also checked, with and without Mn zfs terms. The following notation is used hereafter: $J_{Mn1,Gd} = J_1$, $J_{Mn2,Gd} = J_2$ (when $J_{Mn1,Gd} = J_{Mn2,Gd}$ is assumed, $J_1 = J_2$, $=J$); $J_{Mn1,Mn2} = j$ [$j = 0$ was found at fit 1 (see below) and then always assumed]; $D_{Mn1} = D_1$, $D_{Mn2} = D_2$ (when $D_{Mn1} = D_{Mn2}$ is assumed, $D_1 = D_2$, $= D$), $D_{Gd} = D_3$; $E_{Mn1} = E_1$, $E_{Mn2} = E_2$, $E_{Gd} = E_3$, $g_{Mn1} = g_{Mn2} = g_{Gd} = g$ was always assumed. In order to avoid overparametrization, we considered the following parameters as variable in the eleven successive fits summarized hereafter (those not mentioned were set to zero): fit 1 [J, j and g], fit 2 [J_1, J_2 and g], fit 3 [J, D and g], fit 4 [J, D_1, D_2 and g], fit 5 [J_1, J_2, D and g], fit 6 [J_1, J_2, D_1, D_2 and g], fit 7 [J_1, J_2, D_1, D_2, E and g], fit 8 [J_1, J_2, D_1, D_2, E_2 and g], fit 9 [J_1, J_2, D_1, D_2, D_3 and g], fit 10 [J_1, J_2, D, D_3 and g], fit 11 [J_1, J_2, D_3, E_3 and g]. The agreement factor $R = \Sigma[(\chi_M T)_{obsd.} - (\chi_M T)_{calcd.}]^2 / \Sigma[(\chi_M T)_{obsd.}]^2$ was better by one order of magnitude for fit 8 (2×10^{-5}) compared to fits 1–7 and 9–11 ($1–5 \times 10^{-4}$ range). The parameter values for fit 8 are: $J_1 = 0$, $J_2 = 0.78$ cm^{-1}, $D_1 = 0.14$ cm^{-1}, $D_2 = 0.59$ cm^{-1}, $E_2 = 0.1$ cm^{-1}, $g = 2.02$. As seen in Figure 3, this final fit yielded an excellent agreement between experimental and theoretical $\chi_M T$ values over the whole temperature range.

Comparison of calculated and experimental magnetization at 2 K confirms the assumptions made for fitting the magnetic susceptibility data. The Brillouin functions computed from the parameter values resulting from the fits reported above clearly show that the function corresponding to a unique J parameter (fit 1) does not fit at all the experimental magnetization data (Figure 4, dashed line). Using two different J values (fit 2) yields a better result (dotted line); however, introduction of D_1, D_2 and E_2 zfs terms (fit 8) is needed to obtain a satisfactory agreement between experimental and theoretical magnetization data (solid line). Surprisingly, the data given by fits taking into account gadolinium zfs terms (fits 9–11) are not able to reproduce the experimental magnetization data.

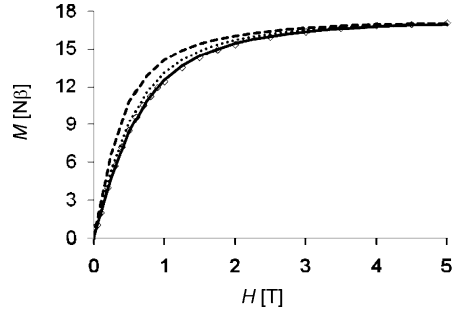

Figure 4. Field dependent magnetization for complex **1** at 2 K. The lines correspond to the Brillouin functions (see text) with a unique J parameter (fit 1, dashed line), J_1 and J_2 (fit 2, dots) and J_1, J_2, D_1, D_2 and E_2 (fit 8, solid line).

Discussion

We successfully prepared and characterized the first manganese–gadolinium–Schiff base complex by using a strictly anaerobic atmosphere. The structural determination confirms that two LMn^{II} units auto-assemble around the gadolinium ion to yield a heterotrinuclear Mn–Gd–Mn complex. This behaviour seems to be contradictory to previous results suggesting that it was not possible to obtain trinuclear 3d-4f-3d entities with nitrato anions.[27] Nevertheless, this apparent contradiction may be removed by taking into account the role of solvents. Nitrato anions are good chelating agents toward lanthanide ions, mainly in acetone where $Gd(NO_3)_3 \cdot 5H_2O$ is a nonelectrolyte; however, it behaves as a 2:1 electrolyte in methanol, implying that only one NO_3 is coordinated to Gd in methanol versus three in acetone. Consequently, in methanol, the solvent used in the present synthetic pathway, the chelating competition between the outer O_2O_2 coordination site of the LMn^{II} unit

and two nitrato ions turns to favour the LMn^{II} complex ligand, yielding the MnOOGdOOMn core. As a result, two nitrato anions are available as ancillary ligands for the Mn centres: one of them chelates Mn2, whereas the other one coordinates Mn1 through O5. Eventually, each Mn ion has two Mn–O(nitrato) bonds, originating either from the same NO_3 or from two different NO_3 anions.

We had previously shown the impossibility to obtain a Mn–Ln–Mn complex from a cationic LMn^{III} complex, the only isolated product corresponding to an ionic species, $[(LMn^{III})]^+_2[Gd(NO_3)_5]^{2-}$.[8] This may be readily explained: indeed, it seems difficult to bring two cationic species in close proximity. This is why we repeated the synthesis of the trinuclear $[(NO_3)Mn(L)(\mu\text{-}NO_3)Gd(L)Mn(NO_3)]$ complex **1** anaerobically. Once the yellow crystals appeared in the mother solution, the sample was taken out of the glove box in order to oxidize Mn^{II} to Mn^{III} in the open atmosphere. The yellow crystals disappeared and new dark crystals were obtained. Their structural determination confirmed Mn oxidation but the resulting product corresponds to the monometallic $[LMn(H_2O)_2]NO_3$ complex. Mn ions do not behave as cobalt ions, from which Co^{II}–Gd and Co^{III}–Gd complexes were isolated.[6] This work thus demonstrates for the first time that Mn^{II}–Gd–Schiff base complexes may be prepared and characterized, but that the corresponding Mn^{III}–Gd entities cannot be isolated.

The magnetic study evidences a weak ferromagnetic Mn^{II}–Gd interaction, in accordance with the few Mn–Gd complexes prepared with ligands other than Schiff bases.[13,18] A first observation related to this magnetic behaviour is that Mn–O bond lengths are larger (by ca. 0.1 Å) than equivalent M^{II}–O bonds (M^{II} = Cu, Ni, Co, Fe). Longer Mn–O bond lengths imply weaker Mn–Gd interactions through the Mn···O···Gd bridges. A second explanation originates from theoretical work on Cu–Gd interactions.[28] It has been found that the presence of ferromagnetism in a large majority of Cu–Gd complexes originates from the interaction between the 3d orbitals and the partially occupied 5d-type Gd^{III} atomic orbitals. From quantum chemical calculations within the C_{2v} symmetry, the authors show that the system adopts an orthogonal orbital exchange pathway, with the main interaction operating between $b_2[Cu^{II}L]$ and $a_2[Gd^{III}]$ orbitals. Consequently, if we consider the Mn^{II} complexes it becomes clear that an orthogonal orbital exchange pathway will be automatically reduced because of the occupancy of the five 3d orbitals, at variance with the Ni–Gd–Ni complexes, where only the 3d e_g orbitals are active. This is why we observe a weaker $J_{Mn,Gd}$ interaction: 0.78 cm^{-1} compared to the 4.8 cm^{-1} value for $J_{Ni,Gd}$.[29] In order to understand why two different $J_{Mn,Gd}$ interactions may operate, we shall keep in mind that we previously found a relationship between the J values and the dihedral angles involving the CuOO and GdOO planes of the bridging CuOOGd core in Cu–Gd complexes.[30] The largest values, around 11 cm^{-1}, were found for planar cores corresponding to dihedral angles around 0°.[30] These values decrease to less than 1 cm^{-1} for dihedral angles increasing to about 45°.[31] This is why we think that the magnetic behaviour of complex **1**, characterized by very different dihedral angles [49.8(1) and 3.3(1)°] and different Mn–O bond lengths must be analyzed by considering two J parameters. In addition, we may conclude that the Mn2 centre with its rhombic distortion is the one involved in the larger (if not unique) Mn–Gd interaction.

The experimental magnetization curve (Figure 4) does imply the presence of small zero-field splitting terms, in agreement with the small $\chi_M T$ decrease at low temperature (Figure 3) and the existence of a signal at zero field in the low-temperature X-band EPR spectrum of complex **1** (Figure S1, Supporting Information). From the entire set of considered fits, the only one able to fit correctly the susceptibility and magnetization data is fit 8, giving the following values: $J_1 = 0$, $J_2 = 0.78\ cm^{-1}$, $D_1 = 0.14\ cm^{-1}$, $D_2 = 0.59\ cm^{-1}$, $E_2 = 0.1\ cm^{-1}$, $g = 2.02$. Surprisingly, the data given by fits taking into account gadolinium zfs terms (fits 9–11) yield too large D values, so that the experimental magnetization data cannot be reproduced in a correct way. If the J parameters and particularly the use of two different J values are not questionable, it is more difficult to confirm that the retained solution is unique. Indeed, Mn^{II} and Gd^{III} ions are both S ions that cannot bring large zfs terms. Furthermore, we must keep in mind that the low-temperature X-band EPR spectra are complicated by absorptions originating from Mn^{II}. For this reason, even high-field EPR spectroscopy may not be able to bring supporting information. This is why we consider that, in the present case, taking into account the rhombic distortion of the Mn2 coordination sphere is more significant than considering a Gd zfs term.

Conclusions

We have been able to synthesize a trinuclear complex, $[(NO_3)Mn(L)(\mu\text{-}NO_3)Gd(L)Mn(NO_3)]$, with a tetradentate Schiff base ligand (L) under controlled atmosphere. The trinuclear nature of this complex results from the use of methanol as solvent. Indeed, the gadolinium nitrate reactant is a 2:1 electrolyte in methanol, whereas it is a nonelectrolyte in acetone. Owing to the coordination of a unique nitrato to gadolinium in methanol, two LMn units behave as ligands with their O_2O_2 outer coordination sites chelating the central Gd ion. This behaviour is favoured by the nitrate affinity for Mn^{II} ions, each nitrato being coordinated to one Mn^{II} ion by at least one Mn–O bond. The structural determination evidences that the Mn–Gd components of complex **1** are nonsymmetric, the dihedral angles between the MnOO and GdOO planes of the Mn1–O_2–Gd and Mn2–O_2–Gd components of the core being equal to 49.8(1) and 3.3(1)°, respectively. The magnetic study confirms the presence of a weak Mn2–Gd ferromagnetic interaction and the absence of measurable magnetic interaction in the Mn1–Gd component of the trinuclear complex. In a previous work describing trinuclear Ni–Gd–Ni entities, the involvement of the 5d orbitals of Gd was put forward. Although the trinuclear Mn–Gd–Mn complex is structurally different from the

Ni–Gd–Ni ones, this involvement does not allow a strict 3d-5d orthogonality here, the five 3d orbitals being occupied in the Mn ions, in agreement with the weaker ferromagnetic $J_{Mn,Gd}$ parameter than $J_{Ni,Gd}$. Mn^{III} ions being involved in a large number of single-molecule magnets (SMM), we tried oxidizing the heteronuclear complex **1** in order to find a new synthetic pathway toward Mn^{III}–Ln entities. Unfortunately, we have not reached this goal, oxidation of Mn^{II} to Mn^{III} being accompanied by release of the 4f ion.

Experimental Section

Materials: The metal salts $Mn(CH_3COO)_2{\cdot}4H_2O$ and $Gd(NO_3)_3{\cdot}5H_2O$ (Aldrich) were used as purchased. High-grade solvents were used for preparing the complexes. The H_2L ligand, *N*,*N*′-2,2-dimethylpropylenebis(3-methoxysalicylideneimine), was prepared as described previously.[32]

Complexes: The reactions and preparation of the samples for physical measurements were carried out under a purified nitrogen atmosphere within a glove box (Vacuum Atmospheres H.E.43.2) equipped with a dry train (Jahan EVAC 7).

$[(NO_3)Mn(L)(\mu\text{-}NO_3)Gd(L)Mn(NO_3)]$ (1): The ligand (0.37 g, 1 mmol) was diluted in dry methanol (20 mL) inside the glove box. Then, manganese acetate (0.25 g, 1 mmol) was added, followed by triethylamine (0.2 g, 2 mmol). An equimolar amount of gadolinium nitrate (1 mmol, 0.45 g) was then added to the stirred mixture, yielding a homogeneous yellow solution. The filtered solution was left to sit for a few days until yellow crystals formed, which were isolated by filtration and dried inside the glove box. Yield: 0.30 g (50%). $C_{42}H_{48}GdMn_2N_7O_{17}$ (1190): calcd. C 42.4, H 4.1, N 8.2; found C 43.9, H 4.0, N 7.7. IR (KBr): $\tilde{\nu}$ = 1627, 1617, 1559, 1465, 1439, 1406, 1313, 1292, 1218, 1060, 968, 849, 737, 637 cm^{-1}.

$[LMn(H_2O)_2](NO_3)(H_2O)_2$ (2): The experimental procedure described above was repeated. The yellow mother solution was taken out of the glove box when the yellow crystals appeared. This mixture was then stirred in the open atmosphere, yielding a dark-brown solution that was concentrated by slow solvent evaporation to yield dark crystals isolated by filtration and dried. Yield: 0.25 g (47%). $C_{21}H_{32}MnN_3O_{11}$ (557.44): calcd. C 45.2, H 5.6, N 7.5; found C 44.8, H 5.7, N 7.2. IR (KBr): $\tilde{\nu}$ = 3364, 2939, 1605, 1557, 1467, 1432, 1412, 1393, 1368, 1348, 1321, 1294, 1247, 1228, 1190, 1164, 1082, 1061, 972, 857, 730, 641 cm^{-1}.

Physical Measurements: Elemental analyses were carried out at the Laboratoire de Chimie de Coordination Microanalytical Laboratory in Toulouse, France, for C, H, and N. IR spectra were recorded with a Spectrum 100 FTIR Perkin–Elmer spectrophotometer using the ATR mode. Magnetic data were obtained with a Quantum Design MPMS SQUID susceptometer. All samples were 3 mm diameter pellets moulded from ground crystalline samples. Magnetic susceptibility measurements were performed in the 2–300 K temperature range in a 0.1 T applied magnetic field, and diamagnetic corrections were applied by using Pascal's constants.[33] Isothermal magnetization measurements were performed up to 5 T at 2 K. The magnetic susceptibilities were computed by exact calculations of the energy levels associated to the spin Hamiltonian through diagonalization of the full-matrix with a general program for axial and rhombic symmetries,[34] and the magnetizations with the MAGPACK program package.[35] Least-squares fittings were accomplished with an adapted version of the function-minimization program MINUIT.[36] Conductivity measurements were obtained with a CRISON 522 conductimeter on 10^{-3} M solutions of $Gd(NO_3)_3{\cdot}6H_2O$ at 25 °C. The results for the molar conductivity Λ_M in acetone and methanol were 10.25 and 167.66 Ω^{-1} cm^2 mol^{-1}, respectively, which corresponds to nonelectrolyte behaviour in acetone and a 2:1 electrolyte in methanol.[37]

Crystallographic Data Collection and Structure Determination: Crystals of **1** and **2** were kept in the mother liquor until they were dipped into oil. The chosen crystals were mounted on a Mitegen micromount and quickly cooled down to 180 K. The selected crystals of **1** (yellow, $0.2 \times 0.18 \times 0.08$ mm^3) and **2** (dark, $0.25 \times 0.1 \times 0.02$ mm^3) were mounted on an Xcalibur Oxford Diffraction diffractometer using a graphite-monochromated Mo-K_α radiation (λ = 0.71073 Å) and equipped with an Oxford Instrument Cooler Device. Data were collected at low temperature (180 K). The final unit cell parameters were obtained by means of a least-squares refinement. The structures were solved by direct methods using SIR92,[38] and refined by means of least-squares procedures on a F_2 with the program SHELXL97[39] included in the software package WinGX version 1.63.[40] The atomic scattering factors were taken from International Tables for X-ray Crystallography.[41] All non-hydrogen atoms were anisotropically refined, and in the last cycles of refinement a weighting scheme was used, where weights are calculated from the following formula: $w = 1/[\sigma^2(F_o^2) + (aP)^2 + bP]$, where $P = (F_o^2 + 2F_c^2)/3$. Drawings of molecules are performed with the program ORTEP32 with 30% probability displacement ellipsoids for non-hydrogen atoms.[42] The crystallographic data of complexes **1** and **2** are summarized in Table 1.

Table 1. Crystallographic data for complexes **1** and **2**.

	1	**2**
Formula	$C_{42}H_{48}GdMn_2N_7O_{17}$	$C_{21}H_{32}MnN_3O_{11}$
Fw	1190.0	557.4
Space group	$P2_1/a$ (N°14)	$C2/c$
a [Å]	16.7761(10)	28.699(10)
b [Å]	11.4808(9)	7.618(5)
c [Å]	24.7443(8)	27.489(5)
α [°]	90	90
β [°]	94.481(6)	125.674(11)
γ [°]	90	90
V [$Å^{-3}$]	4751.3(5)	4882(4)
Z	4	8
$\rho_{calcd.}$ [$g cm^3$]	1.661	1.517
λ [Å]	0.71073	0.71073
T [K]	180(2)	180(2)
μ(Mo-K_α) [mm^{-1}]	1.979	0.606
R[a] obsd., all	0.0458,0.0573	0.0978, 0.128
R*w*[b]obsd., all	0.1062, 0.1133	0.251, 0.1772

[a] $R = \Sigma||F_o| - |F_c||/\Sigma|F_o|$. [b] $wR_2 = [\Sigma w(|F_o^2| - |F_c^2|)^2/\Sigma w|F_o^2|^2]^{1/2}$.

CCDC-730836 (for **1**) and -730837 (for **2**) contain the supplementary crystallographic data for this paper. These data can be obtained free of charge from The Cambridge Crystallographic Data Centre via www.ccdc.cam.ac.uk/data_request/cif.

Supporting Information (see footnote on the first page of this article): Solid state X-band EPR spectrum of complex **1** at 100 K.

Acknowledgments

This work was supported by the European Union Sixth Framework Program NMP3-CT-2005-515767 entitled "MAGMANet: Molecular Approach to Nanomagnets and Multifunctional Materials". The authors are grateful to Dr. A. Mari for technical assistance and to Dr. Juan-Modesto Clemente Juan for helpful discussions.

[1] C. Benelli, D. Gatteschi, *Chem. Rev.* **2002**, *102*, 2369–2387.
[2] M. Sakamoto, K. Manseki, H. Okawa, *Coord. Chem. Rev.* **2001**, *219–221*, 379–414.
[3] R. Gheorghe, P. Cucos, M. Andruh, J. P. Costes, B. Donnadieu, S. Shova, *Chem. Eur. J.* **2006**, *12*, 187–203.
[4] J. P. Costes, S. Shova, J. M. Clemente-Juan, N. Suet, *Dalton Trans.* **2005**, 2830–2832; J. P. Costes, F. Dahan, B. Donnadieu, J. García-Tojal, J. P. Laurent, *Eur. J. Inorg. Chem.* **2001**, 363–365.
[5] J. P. Costes, F. Dahan, A. Dupuis, J. P. Laurent, *Inorg. Chem.* **1997**, *36*, 4284–4286.
[6] J. P. Costes, F. Dahan, J. García-Tojal, *Chem. Eur. J.* **2002**, *8*, 5430–5434.
[7] J. P. Costes, J. M. Clemente-Juan, F. Dahan, F. Dumestre, J. P. Tuchagues, *Inorg. Chem.* **2002**, *41*, 2886–2891.
[8] J. P. Costes, F. Dahan, B. Donnadieu, M. I. Fernandez-Garcia, M. J. Rodriguez-Douton, *Dalton Trans.* **2003**, 3776–3779.
[9] T. Li, S. Gao, B. Li, *Polyhedron* **1998**, *17*, 2243–2248.
[10] Y. J. Kim, Y. J. Park, D. Y. Jung, *Dalton Trans.* **2005**, 2603–2609.
[11] H. L. Gao, B. Zhao, X. Q. Zhao, Y. Song, P. Cheng, D. Z. Liao, S. P. Yan, *Inorg. Chem.* **2008**, *47*, 11057–11061.
[12] B. Zhao, P. Cheng, X. Y. Chen, C. Cheng, W. Shi, D. Z. Liao, S. P. Yan, Z. H. Jiang, *J. Am. Chem. Soc.* **2004**, *126*, 3012–3013; B. Zhao, P. Cheng, Y. Dai, C. Cheng, D. Z. Liao, S. P. Yan, Z. H. Jiang, G. L. Wang, *Angew. Chem. Int. Ed.* **2003**, *42*, 934–936; B. Zhao, H. L. Gao, X. Y. Chen, P. Cheng, W. Shi, D. Z. Liao, S. P. Yan, Z. H. Jiang, *Chem. Eur. J.* **2006**, *12*, 149–158.
[13] T. K. Prasad, M. V. Rajasekharan, J. P. Costes, *Angew. Chem. Int. Ed.* **2007**, *46*, 2851–2854.
[14] C. M. Zaleski, E. C. Depperman, J. W. Kampf, M. L. Kirk, V. L. Pecoraro, *Angew. Chem. Int. Ed.* **2004**, *43*, 3912–3914.
[15] A. Mishra, W. Wernsdorfer, K. A. Abboud, G. Christou, *J. Am. Chem. Soc.* **2004**, *126*, 15648–15649.
[16] B. Wu, *Dalton Trans.* **2006**, 5113–5114.
[17] Y. Bi, Y. Li, W. Liao, H. Zhang, D. Li, *Inorg. Chem.* **2008**, *47*, 9733–9735.
[18] V. Chandrasekhar, B. Murugesa Pandian, R. Boomishankar, A. Steiner, R. Clérac, *Dalton Trans.* **2008**, 5143–5145.
[19] S. Alvarez, D. Avnir, M. Llunell, M. Pinsky, *New J. Chem.* **2002**, *26*, 996–1009.
[20] M. Watkinson, M. Fondo, M. R. Bermejo, A. Sousa, C. A. McAuliffe, R. G. Pritchard, N. Jaiboon, N. Aurangzeb, M. Naeem, *J. Chem. Soc., Dalton Trans.* **1999**, 31–41.
[21] M. Maneiro, M. R. Bermejo, A. Sousa, M. Fondo, A. M. Gonzalez, A. Sousa-Pedrares, C. A. McAuliffe, *Polyhedron* **2000**, *19*, 47–54.
[22] A. Abragam, B. Bleaney, *Electron Paramagnetic Resonance of Transition Ions*, Clarendon Press–Oxford University Press, Oxford, **1969**.
[23] N. Guskos, V. Likodimos, S. Glenis, J. Typek, H. Fuks, M. Wabia, D. G. Paschalidis, D. Tossidis, C. L. Lin, *Eur. Phys. J.* **2002**, *B28*, 277–282.
[24] A. Caneschi, A. Dei, D. Gatteschi, C. A. Massa, L. A. Pardi, S. Poussereau, L. Sorace, *Chem. Phys. Lett.* **2003**, *371*, 694–699.
[25] A. Caneschi, L. Sorace, U. Casellato, P. Tomasin, P. A. Vigato, *Eur. J. Inorg. Chem.* **2004**, 3887–3900.
[26] V. Tangoulis, J. P. Costes, *Chem. Phys.* **2007**, *334*, 77–84.
[27] J. P. Costes, B. Donnadieu, R. Gheorghe, G. Novitchi, J. P. Tuchagues, L. Vendier, *Eur. J. Inorg. Chem.* **2008**, 5235–5244.
[28] J. Paulovic, F. Cimpoesu, M. Ferbinteanu, K. Hirao, *J. Am. Chem. Soc.* **2004**, *126*, 3321–3331.
[29] J. P. Costes, T. Yamagushi, M. Kojima, L. Vendier, *Inorg. Chem.* **2009**, *48*, 5555–5561.
[30] J.-P. Costes, F. Dahan, A. Dupuis, *Inorg. Chem.* **2000**, *39*, 165–168.
[31] G. Novitchi, W. Wernsdorfer, L. F. Chibotaru, J. P. Costes, C. E. Anson, A. K. Powell, *Angew. Chem. Int. Ed.* **2009**, *48*, 1614–1619.
[32] J. P. Costes, J. P. Laussac, F. Nicodème, *J. Chem. Soc., Dalton Trans.* **2002**, 2731–2736.
[33] P. Pascal, *Ann. Chim. Phys.* **1910**, *19*, 5.
[34] A. K. Boudalis, J.-M. Clemente-Juan, F. Dahan, J.-P. Tuchagues, *Inorg. Chem.* **2004**, *43*, 1574–1586.
[35] J. J. Borrás-Almenar, J. M. Clemente-Juan, E. Coronado, B. S. Tsukerblat, *Inorg. Chem.* **1999**, *38*, 6081–6088; J. J. Borrás-Almenar, J. M. Clemente-Juan, E. Coronado, B. S. Tsukerblat, *J. Comput. Chem.* **2001**, *22*, 985–991.
[36] MINUIT – A System for Function Minimization and Analysis of the Parameters Errors and Correlations: F. James, M. Roos, *Comput. Phys. Commun.* **1975**, *10*, 345.
[37] W. J. Geary, *Coord. Chem. Rev.* **1971**, *7*, 81–122.
[38] SIR92 – A Program for Crystal Structure Solution: A. Altomare, G. Cascarano, C. Giacovazzo, A. Guagliardi, *J. Appl. Crystallogr.* **1993**, *26*, 343–350.
[39] G. M. Sheldrick, *SHELX97 – Programs for Crystal Structure Analysis*, release 97–2, Göttingen, Germany, **1998**.
[40] WINGX-1.63 Integrated System of Windows Programs for the Solution, Refinement and Analysis of Single Crystal X-ray Diffraction Data: L. Farrugia, *J. Appl. Crystallogr.* **1999**, *32*, 837–838.
[41] *International Tables for X-ray Crystallography*, Kynoch press, Birmingham, England, **1974**, vol. IV.
[42] ORTEP3 for Windows: L. Farrugia, *J. Appl. Crystallogr.* **1997**, *30*, 565–568.

Received: May 7, 2009
Published Online: July 23, 2009

